

## Current injection and transport in polyfluorene

Chieh-Kai Yang, Chia-Ming Yang, Hua-Hsien Liao, Sheng-Fu Horng, and Hsin-Fei Meng

Citation: *Applied Physics Letters* **91**, 093504 (2007); doi: 10.1063/1.2759951

View online: <http://dx.doi.org/10.1063/1.2759951>

View Table of Contents: <http://scitation.aip.org/content/aip/journal/apl/91/9?ver=pdfcov>

Published by the [AIP Publishing](#)

---

### Articles you may be interested in

Hole transport in the organic small molecule material -NPD : evidence for the presence of correlated disorder  
*J. Appl. Phys.* **107**, 113710 (2010); 10.1063/1.3407561

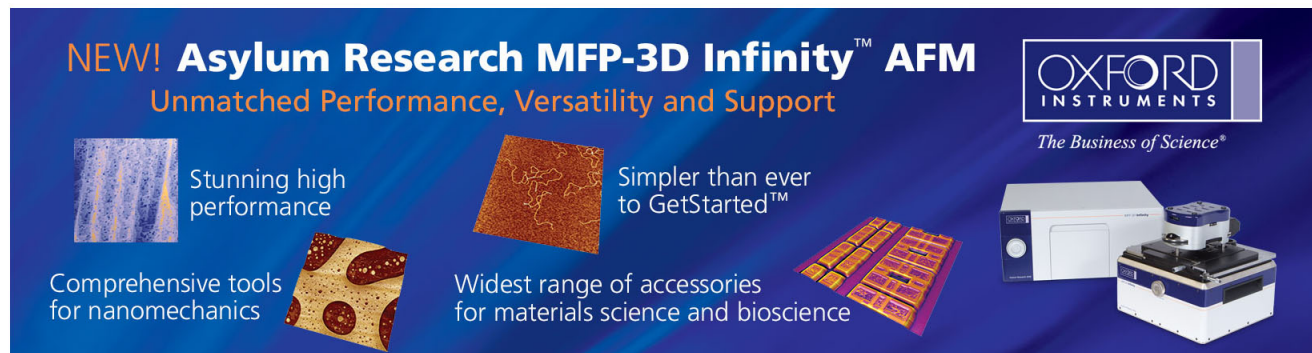
Interdependence of contact properties and field- and density-dependent mobility in organic field-effect transistors  
*J. Appl. Phys.* **105**, 014509 (2009); 10.1063/1.3058640

Ohmic hole injection in poly(9,9-dioctylfluorene) polymer light-emitting diodes  
*Appl. Phys. Lett.* **83**, 707 (2003); 10.1063/1.1596722

Optical properties of single carrier polymer diodes under high electrical injection  
*Appl. Phys. Lett.* **78**, 270 (2001); 10.1063/1.1340859

A numerical study of operational characteristics of organic light-emitting diodes  
*J. Appl. Phys.* **84**, 5306 (1998); 10.1063/1.368779

---

The advertisement features a dark blue background with white and orange text. At the top left, it reads 'NEW! Asylum Research MFP-3D Infinity™ AFM' in large white letters, followed by 'Unmatched Performance, Versatility and Support' in orange. On the right, the Oxford Instruments logo is shown with the tagline 'The Business of Science®'. Below the text are four images: a textured surface, a brown surface with a network of lines, a grid of small rectangular samples, and the MFP-3D Infinity AFM instrument itself. Text descriptions are placed around these images: 'Stunning high performance' next to the first image, 'Simpler than ever to GetStarted™' next to the second, 'Comprehensive tools for nanomechanics' next to the third, and 'Widest range of accessories for materials science and bioscience' next to the fourth.

**NEW! Asylum Research MFP-3D Infinity™ AFM**  
Unmatched Performance, Versatility and Support

**OXFORD INSTRUMENTS**  
The Business of Science®

Stunning high performance

Simpler than ever to GetStarted™

Comprehensive tools for nanomechanics

Widest range of accessories for materials science and bioscience

## Current injection and transport in polyfluorene

Chieh-Kai Yang, Chia-Ming Yang, Hua-Hsien Liao, and Sheng-Fu Horng  
 Department of Electric Engineering, National Tsing Hua University, Hsinchu, 300 Taiwan,  
 Republic of China

Hsin-Fei Meng<sup>a)</sup>

Institute of Physics, National Chiao Tung University, Hsinchu, 300 Taiwan, Republic of China

(Received 11 May 2007; accepted 24 June 2007; published online 28 August 2007)

A comprehensive numerical model is established for the electrical processes in a sandwich organic semiconductor device with high carrier injection barrier. The charge injection at the anode interface with 0.8 eV energy barrier is dominated by the hopping among the gap states of the semiconductor caused by disorders. The Ohmic behavior at low voltage is demonstrated to be not due to the background doping but the filaments formed by conductive clusters. In bipolar devices with low work function cathode it is shown that near the anode the electron traps significantly enhance hole injection through Fowler-Nordheim tunneling, resulting in rapid increases of the hole carrier and current in comparison with the hole-only devices. © 2007 American Institute of Physics. [DOI: 10.1063/1.2759951]

The junction between metal electrode and organic semiconductor is often not Ohmic due to a large charge carrier injection barrier. Even for the interfaces which appear to be Ohmic judged by work function, a barrier may result from Fermi level pinning at the midgap or interface dipoles. Despite of the dominance the larger barrier, so far the comprehensive device models are only based on Ohmic contact involving the conventional injection mechanisms of thermionic and tunneling currents,<sup>1</sup> which both decrease exponentially with the energy barrier. Such model not only usually underestimates the experimental current density but also overestimates the slope of the current-voltage relation. In addition, it predicts a very strong temperature dependence of the current which is never observed.<sup>2</sup> A fundamental modification of the injection model must be made in order to describe the electrical processes in organic semiconductor structures with large energy barriers.

Several mechanisms on the current injection through a large barrier were proposed, including the random hopping due to energy disorders at the interface,<sup>2-5</sup> the background doping,<sup>6</sup> and conducting filaments that act as shorts between the electrodes.<sup>7</sup> They are, however, qualitative disjoint concepts targeted only for specific experimental observations. In this work we formulate a comprehensive model for the charge carrier injection and transport in sandwich organic devices with large injection barrier. The disjoint concepts are systematically incorporated into the boundary conditions and the bulk equations. As we take the wide band gap polymer poly(9,9-dioctylfluorene) (PFO) as the experimental example with high injection barrier of 0.8 eV, the numerical calculation of the model is able to fit quantitatively the measured electrical characteristics for the entire range of voltage for both unipolar and bipolar injections.

At the junction we impose the boundary conditions that the drift-diffusion current matches the interface current including conventionally thermionic emission, backflow surface recombination, and Fowler-Nordheim tunneling.<sup>3-5</sup> As discussed above, for high injection barrier from metal to

semiconductor, the thermionic and tunneling currents are both too small to account for the observed current density. Instead of injecting directly into the band edge, the current is dominated by random hopping among localized level within the gap due to disorders which are closer to the electrode Fermi level. The boundary condition becomes

$$J_{\text{dev}} = AT^2 \exp\left(-\frac{\phi_{\text{eff}}}{kT}\right) - \frac{AT^2}{N_{c(v)}} n_j(p_j) + \frac{e}{16\pi^2\hbar\phi_{\text{eff}}} E^2 \exp\left(-\frac{4\sqrt{2m}\phi_{\text{eff}}^{3/2}}{3\hbar E}\right) + J_{\text{hop}}, \quad (1)$$

where  $J_{\text{dev}} = en\mu_n E + eD_n(dn/dx)$  for electron and  $J_{\text{dev}} = ep\mu_p E - eD_p(dp/dx)$  for hole. The mobility is given by  $\mu = \mu^* \exp(-\Delta/kT) \exp\{B[(1/kT) - (1/kT_0)]\sqrt{E}\}$  with  $\Delta = 0.5$  eV,  $T_0 = 500$  K, and  $\mu^*$  and  $B$  are separate adjustable parameters for electron and hole. The Richardson constant is  $A = 120 \text{ A/cm}^2 \text{ K}^2$ .  $\phi_{\text{eff}}$  is the effective energy barrier and equal to  $\phi_{\text{eff}} = \phi_B - \sqrt{eE/4\pi\epsilon}$  with image force lowering where  $\phi_B$  is the original energy barrier,  $N_{c(v)}$  is effective density of states in the conduction (valence) band,  $n_j(p_j)$  the electron (hole) density at the interface,  $\hbar$  the Planck constant, and  $m$  the effective carrier mass. The first three terms in Eq. (1) are thermionic, backflow, and tunneling currents, respectively. The fourth term is given by the hopping current given by Arkhipov and coworkers,<sup>5</sup> with parameters including the distance  $a$  from the electrode to the first available hopping site in the bulk, the attempt-to-jump frequency  $\nu_0$ , the inverse localization radius  $\gamma$ , and density of states energy width  $\sigma$ .

The electron traps are included in the model following previous works.<sup>8</sup> The trap density is assumed to be exponential  $n_t(\epsilon) = (N_t/kT) \exp[(\epsilon - E_c/kT)]$ , with  $n_t(\epsilon)$  the trap density of states at energy  $\epsilon$ ,  $E_c$  the energy of the conduction band,  $N_t$  the total density of traps, and  $kT$ , an energy characterizing the trap distribution.

At low voltage below the flat-band condition there is an Ohmic region. Background doping is included in the model since its density may be higher than the injected space charge at such voltages. The Poisson equation is modified accordingly. Another process at low voltage region is the formation

<sup>a)</sup> Author to whom correspondence should be addressed; electronic mail: meng@mail.nctu.edu.tw

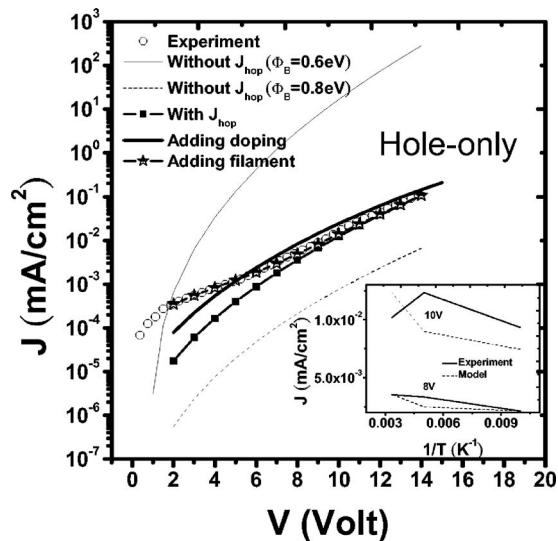


FIG. 1. Injection limited hole current  $J$  is plotted against applied voltage  $V$  for a PEDOT:PSS/PFO/Au hole-only device at temperature of 300 K. The hole injection barrier  $\phi_B$  is 0.8 eV for all model calculation except the thin solid line. The model calculated  $J$ - $V$  characteristics with different current contributions at low applied voltage are plotted as dashed line (without  $J_{\text{hop}}$ ), square line [(with  $J_{\text{hop}}$ ), solid line (adding  $2.2 \times 10^{16} \text{ cm}^{-3}$   $p$ -doping density), and star line (adding filament conduction  $\rho = 7.58 \times 10^{11} \Omega$ )]. The inset shows measured and calculated currents at 8 and 10 V with three different temperatures of  $T = 100, 200,$  and  $300 \text{ K}$ .

of conducting filaments,<sup>9</sup> possibly caused by the percolation path of metallic clusters coming from the electrodes. The filament current is  $J_f = V/\rho_f$ , where  $\rho_f$  the filament resistance.  $J_f$  is added to the current calculated from the device model to obtain the total current. The numerical procedure to obtain the steady state solution and device current at a given voltage have been described previously.<sup>8</sup>

The model predictions are compared with various device structures based on the wide gap polymer PFO. The structure of the hole-only device is PEDOT:PSS/PFO/Au. The PFO thickness is fixed at 100 nm for all cases. The anode PEDOT:PSS is poly(3,4-ethylenedioxythiophene) doped with poly(styrenesulfonate) with work function of 5.2 eV. The hole mobility of PFO is not taken as a fitting parameter but independently measured by transient electroluminescence. Our result is  $\mu^* = 2.3 \times 10^3 \text{ cm}^2 \text{ V}^{-1} \text{ s}^{-1}$  and  $B = 8.4 \times 10^{-5} \text{ eV}^{1/2} \text{ cm}^{1/2}$ . The parameters related to the conventional interface currents including thermionic, backflow, and tunneling are the same as the ones used for low injection barrier cases.<sup>8</sup> The model parameters are electron affinity = 2.6 eV, ionization potential = 6.0 eV,  $n_{c(v)} = 10^{21} \text{ cm}^{-3}$ , and relative dielectric constant  $\epsilon = 3$ . Ignoring doping, filaments, and random hopping to the gap states the model current is shown as dashed line in Fig. 1 which is far smaller than the experiments. As the random hopping is incorporated in the model, with parameters  $\gamma = 3.1 \times 10^{-7} \text{ cm}^{-1}$ ,  $\sigma = 0.149 \text{ eV}$ ,  $a = 1.67 \text{ nm}$ , and  $v_0 = 1 \times 10^{12} \text{ s}^{-1}$ , the current-voltage relation becomes very close to the experiment except for low voltage region. Note this is not achieved by adjusting the hole mobility  $\mu_h$  as the fitting parameter. The temperature dependence of device current is shown in the inset of Fig. 1. The weak temperature dependence for both model and experiments indicates that the injection does not require the thermal activation across the large barrier, supporting the picture of hopping through gap states. Moreover, the current-voltage ( $JV$ ) relation does not show up as straight in the Flower-

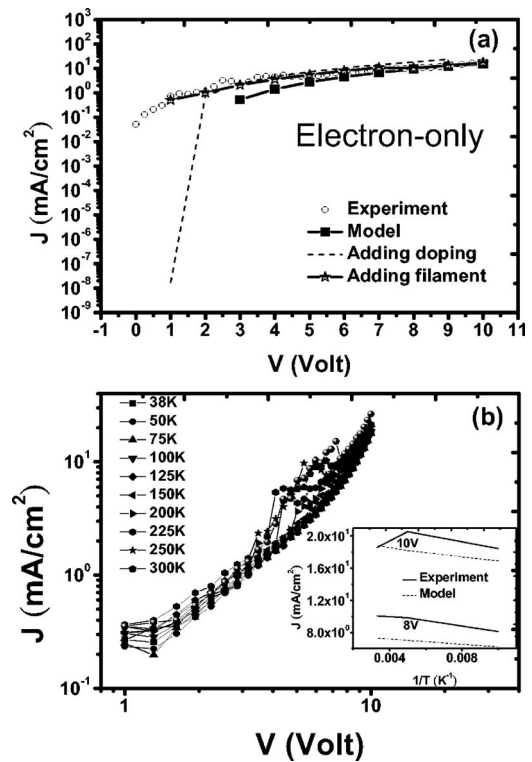


FIG. 2. (a) Space charge limited electron current  $J$  vs applied voltage  $V$  for an Al/PFO/CsF/Al electron-only device at 300 K. The model calculated  $J$ - $V$  characteristics with different current contributions at low applied voltage are plotted as square line (without filament conduction), star line (with filament conduction  $\rho = 5.0 \times 10^4 \Omega$ ), and dashed line ( $1.0 \times 10^{17} \text{ cm}^{-3}$   $n$  doping). (b) Measured  $J$ - $V$  characteristics with different temperatures from 300 to 38 K. The inset shows measured and calculated currents at 8 and 10 V with three different temperatures of 100, 200, and 300 K.

Nordheim plot,<sup>2</sup> indicating that tunneling is not the main injection channel. If we remove  $J_{\text{hop}}$  and reduce the barrier to 0.6 eV, the model current will be raised but the  $JV$  slope becomes far larger than the experiment as shown in Fig. 1. Hopping to the gap states is therefore identified as the correct injection mechanism except for low voltage.

One possible explanation for the large discrepancy in the  $JV$  relation at low voltages in Fig. 1 is the effect of background doping.<sup>6</sup> However, it turns out that even for doping as high as  $2.2 \times 10^{16} \text{ cm}^{-3}$  the model prediction of the current is still too low, as shown by the thick solid line in Fig. 1. Raising the doping further would be unphysical. We therefore employ the filament term to describe the low voltage  $JV$ . Indeed the entire  $JV$  curve can be described by adding the filament contribution. The quantitative agreement between the model and the experiments establishes that for unipolar device the current is dominated by the hopping into the random disorder sites below the band edge at moderate to high voltage, while it is dominated by the arbitrary filament conduction channels instead of the semiconductor background doping in the low voltage region.

In order to describe the bipolar operation we first study the model for electron-only current. The current-voltage plot for the Al/PFO/CsF/Al electron-only device is shown in Fig. 2(a). The Fermi level of cathode is pinned at the conduction band edge. The thermionic and backflow nearly cancel each other to establish a local thermal equilibrium. In such contact the random hopping term makes no contribution to the injection.<sup>3</sup> The total current is expected to follow a space-charge-limited current (SCLC) with quadratic  $JV$  rela-



tion. Since the electron mobility in PFO can hardly be measured experimentally,  $\mu_n$  is obtained by  $JV$  fitting which gives  $\mu^* = 7.485 \times 10^2 \text{ cm}^2 \text{ V}^{-1} \text{ s}^{-1}$  and  $B = 2.1 \times 10^{-5} \text{ eV}^{1/2} \text{ cm}^{1/2}$ . The calculated result (square line) shows a quadratic SCLC characteristics and agrees with the experiments (circle) at higher voltage. The discrepancy at low voltage cannot be described by the doping up to  $2.2 \times 10^{16} \text{ cm}^{-3}$ , as shown in Fig. 2(a) (dashed line). This suggests that, as the case of hole-only current, filaments dominate the low voltage current. Indeed as we add the filament contribution there is a good fitting (star line) for the entire voltage range, as shown in Fig. 2(a). The currents in Al/PFO/CsF/Al device exhibit a very weak temperature dependence, as shown in Fig. 2(b). A good agreement shown in the inset is obtained by taking the mobility as temperature independent. The independence may result from the high electron density which smoothes the potential variation and reduces the energy disorders. Because of the lack of a large barrier, the electron-only current turns out to be larger than the hole-only current by three orders of magnitude despite of the lower mobility. Yet the PFO LED is known to possess a large hole current. The hole injection must be enhanced under bipolar operation.

The bipolar device structure is PEDOT:PSS/PFO/Ca/Al. The recombination rate  $R$  is given by  $R = \gamma np$ , where  $n$  and  $p$  are electron and hole densities, respectively.  $\gamma = (e/\epsilon_r \epsilon_0)(\mu_n + \mu_p)$  is the Langevin recombination coefficient. The parameters for hole-only and electron-only devices remain the same. Without any free parameter the calculated  $JV$  relation is shown to have excellent agreement with the bipolar experiment in Fig. 3(a) from 0 to 8 V. There is nevertheless an underestimation for the current at voltages over 8 V. Electron traps near the PEDOT:PSS/PFO interface, due to the segregation of PSS from PEDOT:PSS,<sup>10</sup> were shown to enhance the hole injection from the anode.<sup>7,10,11</sup> Adding electron traps with concentration of  $3 \times 10^{18} \text{ cm}^{-3}$  that distribute over 10 nm from the anode, a good agreement is shown in Fig. 3(a) (star line). Figure 3(b) shows the effect of trapped electrons in detail. The more the trapped electrons near the interface, the stronger the electric field at the anode, causing the tunneling of holes and an increase in hole density. With applied voltages from 8 to 10 V the increased hole carriers contribute to the recombination with electrons near the interface and reduce the number of trapped electrons, as shown in Fig. 3(b). The inset shows the hole and electron densities as functions of the voltage. The electron density increases linearly with the voltage which is the characteristic for SCLC. On the other hand, the hole density increases exponentially, the characteristic of a junction limited injection. The total current  $J_{\text{dev}}$  can be decomposed as  $J_{\text{dev}} = J_h^a + J_e^c - J_R$ , where  $J_h^a$  is the hole current at the anode,  $J_e^c$  is the electron current at the cathode, and  $J_R$  is the integrated recombination current. The three components are plotted in Fig. 3(a). Despite of the large barrier,  $J_h^a$  is now comparable to  $J_e^c$  at high voltages due to the enhancement of electron traps and renders the light-emitting diode a reasonable efficiency.

In conclusion, we establish a device model for a sandwich organic device with large injection barrier. The prediction on the current-voltage relation is in excellent agreement

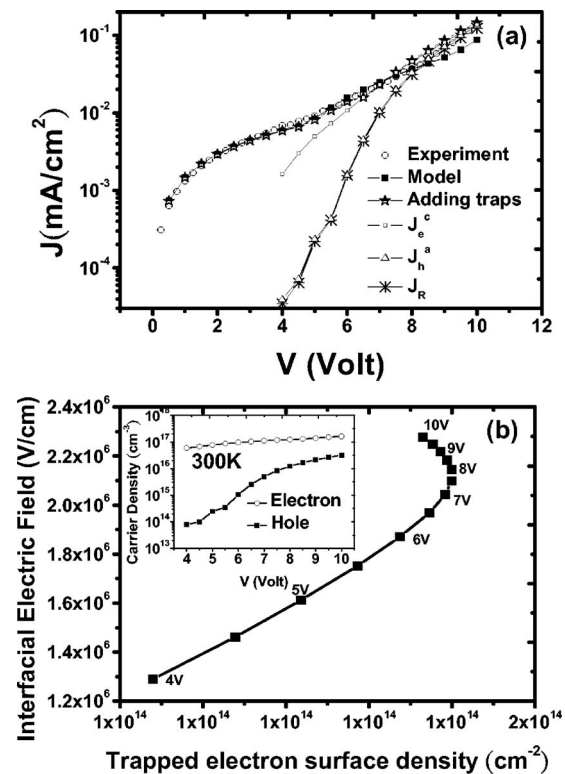


FIG. 3. (a) Light-emitting diode current  $J$  vs applied voltage  $V$  for a PEDOT:PSS/PFO/Ca/Al bipolar device at 300 K. The model calculated  $J$ - $V$  characteristics are plotted as square line (without electron traps and with filament conduction), star line (with  $3.0 \times 10^{18} \text{ cm}^{-3}$  electron traps distributed over 10 nm from the anode and with filament conduction), hollow-square line (electron current at cathode without filament conduction), hollow-triangle line (hole current at anode without filament conduction), and snowflake line (recombination current without filament conduction). (b) Calculated electric field at the interface of PEDOT:PSS/PFO vs total trapped electrons for the PEDOT:PSS/PFO/CaAl device at 300 K. The inset shows the calculated total carrier numbers as function of the applied voltage.

with the experiments for the entire voltage range and for unipolar as well as bipolar devices. With large barrier the holes are injected through the random sites within the gap. In bipolar devices the trapped electrons further enhance the hole currents by reducing the tunneling barrier.

This work was supported by the National Science Council of the Republic of China.

- <sup>1</sup>P. S. Davids, I. H. Campbell, and D. L. Smith, *J. Appl. Phys.* **82**, 12 (1997).
- <sup>2</sup>S. Barth, U. Wolf, H. Bässler, P. Müller, H. Riel, H. Vestweber, P. F. Seidler, and W. Rieb, *Phys. Rev. B* **60**, 8791 (1999).
- <sup>3</sup>T. van Woudenberg, P. W. M. Blom, M. C. J. M. Vissenberg, and J. N. Huiberts, *Appl. Phys. Lett.* **79**, 1697 (2001).
- <sup>4</sup>V. I. Arkhipov, E. V. Emelianova, Y. H. Tak, and H. Bassler, *J. Appl. Phys.* **84**, 2 (1998).
- <sup>5</sup>V. I. Arkhipov, U. Wolf, and H. Bassler, *Phys. Rev. B* **59**, 11 (1999).
- <sup>6</sup>S. C. Jain, W. Geens, A. Mehra, V. Kumar, T. Aernouts, J. Poortmans, R. Mertens, and M. Willander, *J. Appl. Phys.* **89**, 3804 (2001).
- <sup>7</sup>P. J. Brewer, P. A. Lane, J. Huang, A. J. deMello, D. D. C. Bradley, and J. C. deMello, *Phys. Rev. B* **71**, 205209 (2005).
- <sup>8</sup>M. J. Tsai and H. F. Meng, *J. Appl. Phys.* **97**, 114502 (2005).
- <sup>9</sup>S. Gravano, E. Amr, R. D. Gould, and M. Abu Samrab, *Thin Solid Films* **433**, 321 (2003).
- <sup>10</sup>T. van Woudenberg, J. Wildeman, P. W. M. Blom, J. J. A. M. Bastiaansen, and Bea M. W. Langeveld-Voss, *Adv. Funct. Mater.* **14**, 677 (2004).
- <sup>11</sup>P. J. Brewer, J. Huang, P. A. Lane, A. J. deMello, D. D. C. Bradley, and J. C. deMello, *Phys. Rev. B* **74**, 115202 (2006).